Journal of Molecular Liquids 309 (2020) 113110

Contents lists available at ScienceDirect

Journal of Molecular Liquids

journal homepage: www.elsevier.com/locate/molliq

Experimental and predicted physicochemical properties of monopropanolamine-based deep eutectic solvents

Bartosz Nowosielski [a], Marzena Jamrógiewicz [c], Justyna Łuczak [b], Maciej Śmiechowski [a], Dorota Warmińska [a,*]

[a] Department of Physical Chemistry, Faculty of Chemistry, Gdańsk University of Technology, ul. Narutowicza 11/12, 80-233 Gdańsk, Poland
[b] Department of Process Engineering and Chemical Technology, Faculty of Chemistry, Gdańsk University of Technology, ul. Narutowicza 11/12, 80-233 Gdańsk, Poland
[c] Department of Physical Chemistry, Faculty of Pharmacy, Medical University of Gdańsk, Al. Gen. Hallera 107, 80-416 Gdańsk, Poland

ARTICLE INFO

Article history:
Received 19 February 2020
Received in revised form 2 April 2020
Accepted 7 April 2020
Available online 11 April 2020

Keywords:
DES
3-amino-1-propanol
Tetraalkylammonium salts
Physicochemical properties

ABSTRACT

In this work, the novel deep eutectic solvents (DESs) based on 3-amino-1-propanol (AP) as hydrogen bond donor (HBD) and tetrabutylammonium bromide (TBAB) or tetrabutylammonium chloride (TBAC) or tetraethylammonium chloride (TEAC) as hydrogen bond acceptors (HBAs) were synthesized with different molar ratios of 1: 4, 1: 6 and 1: 8 salt to AP. Fourier Transform Infrared Spectroscopy measurements were performed to provide an evidence of any chemical structure changes. Physical properties of the prepared DESs including densities, viscosities, refractive indices and sound velocities were measured within the temperature range of 293.15–333.15 K at the pressure of 0.1 MPa. They were analyzed in terms of estimating the effect of HBA to HBD molar ratio, anion and length of alkyl chain in a salt, and their temperature dependences were fitted by empirical equations. Thermal expansion coefficients and activation energies for viscous flow were obtained accordingly. Moreover, experimental values of density and refractive index were compared with predicted ones. For prediction of density, Rackett equation modified by Spencer and Danner and the mass connectivity index-based method were used, while refractive index was estimated by the atomic contribution method.

1. Introduction

One of the main directions of global research nowadays is the search for technologies aimed at reducing carbon dioxide emissions. This gas, mainly responsible for the occurrence of the greenhouse effect, is emitted to the atmosphere in the processes of electricity and heat production based on fossil combustion [1]. In power plants, due to the low pressure of flue gases, one of the most common technologies used for CO_2 removal is absorption using aqueous amine solutions. The highest efficiency of the CO_2 removal process is achieved by chemical absorption using a 30% aqueous solution of monoethanolamine (MEA) [2]. However, the corrosive nature of the reaction environment and its loss due to volatility make it desirable to search for alternative solvents that could replace aqueous solutions of MEA or other alkanolamines.

Since 2008, attempts have been noted in the literature to use deep eutectic mixtures for the removal of CO_2 from industrial process streams [3]. These solvents have similar physical properties as ionic liquids, are practically non-volatile and non-flammable, and exhibit high thermal and electrochemical stability, but are definitely cheaper, less toxic and often biodegradable [4–9]. As with ionic liquids, their physical properties can be controlled by changing the composition and proportions of the components making up a given eutectic mixture, so as to obtain advantageous properties for a specific application.

The research performed so far clearly shows that the solubility of carbon dioxide depends on the structure of a deep eutectic mixture, which determines not only the chemical properties of the solvent (the possibility of chemisorption or the lack thereof), but also its physical properties, including viscosity—a key parameter in the technological process [10]. It has been established, that DESs based on alkanolamines have much higher CO_2 absorption capacity than other deep eutectic solvents, for which no chemical reactions with carbon dioxide are observed [7,10]. So far, deep eutectic solvents with monoethanolamine [10–12], diethanolamine [10,12,13], triethanolamine [14] and methyldiethanolamine [10,12,13] as hydrogen bond donor and DESs based on monoethanolamine chloride [7] or *N,N*-diethylenethanolammonium chloride [14] as hydrogen bond acceptor have been studied. For these systems the physical properties such as density, viscosity, surface tension and refractive index have been determined.

In this study, novel deep eutectic solvents were prepared by introducing 3-amino-1-propanol (AP), which is a good CO_2 absorbent, as a hydrogen bond donor (HBD) coupled with tetrabutylammonium bromide (TBAB) or tetrabutylammonium chloride (TBAC) or tetraethylammonium chloride (TEAC) as hydrogen bond acceptors (HBAs). The DESs were obtained for three different salts to amine

* Corresponding author.
E-mail address: dorwarmi@pg.edu.pl (D. Warmińska).

https://doi.org/10.1016/j.molliq.2020.113110
0167-7322/

molar ratios of 1:4, 1:6 and 1:8 and characterized by measuring their main physical properties such as density, viscosity, refractive index and sound velocity at temperatures from 293.15 to 333.15 K. Temperature dependences of physical properties were fitted by empirical equations, and both thermal expansion coefficients or activation energies for viscous flow were obtained accordingly. Moreover, Rackett equation modified by Spencer and Danner and the mass connectivity index-based method were used for density prediction, while the refractive index was estimated by the atomic contribution method. The influence of the size of tetraalkylammonium cation as well as the type of anion of salt on physical properties of DESs and the strength of hydrogen bond interactions between HBA and HBD were discussed.

2. Experimental

2.1. Chemicals and synthesis

The chemicals in this study, 3-amino-1-propanol, tetrabutylammonium bromide, tetrabutylammonium chloride and tetraethylammonium chloride were purchased from Sigma-Aldrich and apart from TBAC they were used as received from the supplier. Tetrabutylammonium chloride was purified by double crystallization from acetone by adding diethyl ether. All salts were dried under reduced pressure before use, TBAB at 323 K for 48 h, TBAC and TEAC at 298.15 K for several days. The corresponding information and the chemical structures of the DESs ingredients are presented in Table 1 and Fig. 1, respectively.

In this work, DESs were prepared by mass with the same molar ratio of 1:4, 1:6 and 1:8 salt to 3-amino-1-propanol. The weighing was done using an analytical balance (Mettler Toledo) with the precision of 0.1 mg. The standard uncertainty in the mass fraction was estimated to be less than $\pm 1 \cdot 10^{-4}$. The combinations of the quaternary salts and AP were mixed at 353.15 K for 1 h using a magnetic stirrer in a fume hood until a homogeneous and uniform liquid without any precipitate was formed. This is commonly described as the heating method of DES formation [15]. The final DESs, stable colourless liquids at room temperature, were kept in tight bottles to prevent any contamination from outside atmosphere that may affect the physical properties of DES. Since deep eutectic solvents are known as hygroscopic solvents, the water content of DESs was measured using a Mettler Toledo Coulometric Karl - Fischer titrator (899 Coulometer apparatus from Metrohm), as presented in Table 2.

2.2. Physical properties measurements

2.2.1. Melting point

Mettler Toledo Star One Differential Scanning Calorimeter (DSC) was used to measure the melting points of the eutectic mixtures. The measurements were made under purified nitrogen atmosphere with a flow rate of 60 $mL \cdot min^{-1}$, with samples of 10–18 mg packed in standard aluminium pan. The DSC equipment was connected to the STAR® data acquisition software a dedicated computer. The heating and cooling sequence was programmed on the STAR® console which controls the DSC equipment. For the melting point determination, a temperature range from 193.15 to 298.15 K was selected with a heating rate of 1 $K \cdot min^{-1}$. The uncertainty of the measurement was ±0.01 K. This procedure was performed in at least three repetitions to ensure reproducibility of the results.

2.2.2. Density

The densities of the DES samples were measured at different temperatures with a digital vibration-tube analyser (Anton Paar DMA 5000, Austria) with proportional temperature control that kept the samples at working temperature with an accuracy of ±0.01 K. The apparatus was calibrated with double distilled, deionized and degassed water, and with dry air at atmospheric pressure (0.1 MPa) according to the apparatus catalogue. The standard uncertainty of density measurement was better than 0.35 $kg \cdot m^{-3}$.

2.2.3. Sound velocity

The sound velocities were determined using the sound analyser OPTIME 1.0 from OPTEL (Poland) with the standard uncertainty of 0.5 $m \cdot s^{-1}$ by measuring the time it takes for a pulse of ultrasound to travel from one transducer to another (*pitch-catch*) or to return to the same transducer (*pulse-echo*). The cell was thermostated at 298.15 ± 0.01 K and calibrated with double distilled water, with the value 1496.69 $m \cdot s^{-1}$ used as the sound velocity in pure water at 298.15 K.

2.2.4. Viscosity

Viscosities of the solvents were determined using LVDV-III Programmable Rheometer (cone-plate viscometer; Brookfield Engineering Laboratory, USA), controlled by a computer. The temperature of the samples was controlled within ±0.01 K using a thermostatic water bath (PolyScience 9106, USA). The display of the viscosimeter was verified with certified viscosity standard N100 and S3 provided by Cannon at 298.15 ± 0.01 K. The standard uncertainty of viscosity measurement was better than 1%.

2.2.5. Refractive index

The refractive indices were measured using an Abbe refractometer (RL-3, Poland) equipped with a thermostat for controlling the cell temperature with an accuracy of ±0.1 K. The standard uncertainty of refractive index measurement on the n_D scale was 0.0002. At least three independent measurements were taken for each sample at each temperature to assure reproducibility of the measurement.

2.2.6. Infrared spectroscopy measurements

FTIR spectra of DESs were recorded on Nicolet 8700 spectrometer (Thermo Electron Co.). An attenuated total reflection (ATR) technique was employed because of extremely strong absorption of AP for $\nu(OH)/\nu(NH_2)$ stretching vibrations. For this purpose, the Specac Golden Gate single reflection accessory equipped with a diamond crystal (45° incidence angle) mounted in a heated tungsten carbide disc was used. The temperature of the 50 mL liquid sample cell atop the crystal was kept at 298.15 ± 0.1 K by the Specac West 6100+ controller maintaining the tungsten carbide disc temperature and additionally stabilized by circulating thermostated water from a Julabo F12 thermostat. The sample temperature was monitored by a thermocouple inside the cell. The spectrometer measurement chamber and the ATR accessory were purged with dry nitrogen. The sample spectra were ratioed against a background spectrum collected for an empty, dry cell obtained

Table 1
Provenance and mass fraction purity of the compounds studied.

Chemical name	Source	CAS number	Initial purity/mass fraction[a]	Purification method	Final purity/mass fraction[a]
3-amino-1-propanol (AP)	Sigma Aldrich	156-87-6	0.99	None	–
Tetrabutylammonium bromide (TBAB)	Sigma Aldrich	1643-19-2	≥0.99	None	–
Tetraethylammonium chloride (TEAC)	Sigma Aldrich	56-34-8	≥0.98	None	–
Tetrabutylammonium chloride (TBAC)	Sigma Aldrich	1112-67-0	≥0.97	Crystalization	≥0.98[b]

[a] As stated by the supplier.
[b] Determined by potentiometric titration.

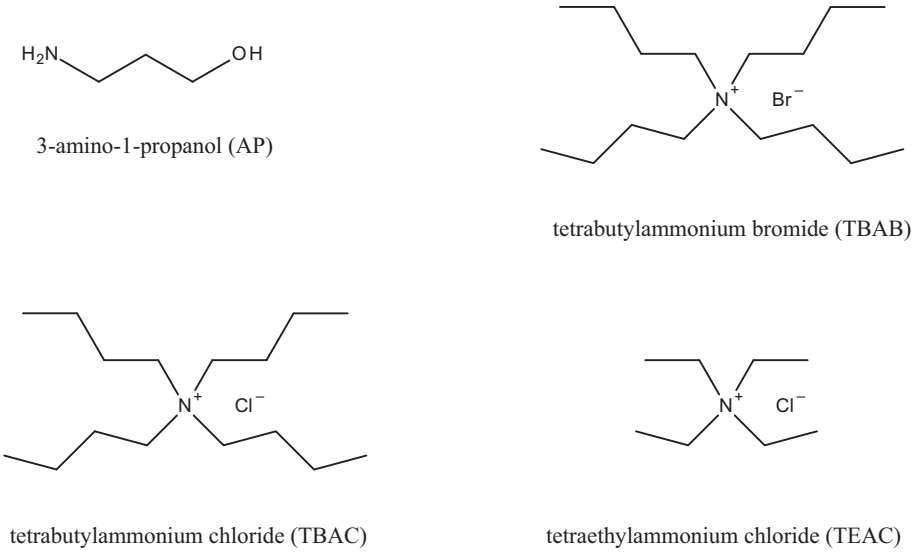

Fig. 1. Chemical structures of the DESs ingredients used in this study.

directly before each measurement. For each sample spectrum 256 scans were performed with a selected resolution of 2.0 cm^{-1}.

Spectra acquisition was controlled by OMNIC 7.3 software package (Thermo Scientific). Advanced ATR correction algorithm of the software was used to correct for normal and anomalous dispersion effects. It requires the knowledge of the crystal material, the incidence angle, the number of internal reflections and the refractive index of the sample. The spectra were further analyzed using GRAMS/32 software (Galactic Industries Corp.).

3. Results and discussion

3.1. Melting point

Differential scanning calorimetry (DSC) was used to determine the melting point and any solid state phase transitions in the present of quaternary DESs. The heating rate of 1 $K \cdot min^{-1}$ was used to increase the sensitivity of the instrument. Table 2 shows the melting points of DES. Fig. 2 (a,b,c) illustrates DSC curves for the DES systems with three HDA:HBD ratios. DSC plots for the eutectic mixtures were collected for at least three runs to ensure the reproducibility. Generally, only one endothermic peak was identified which was considered as the melting peak, but in the case of TBAB - AP 1:8 we observed a doublet form of melting peak. No phase transition peak was observed. The melting temperature in the present work is taken as the peak temperature in the heating profile. For all the studied DESs the melting points were lower than for the pure components. Moreover, the order of melting temperatures for DES at the same molar ratio of the salt to 3-amine-1-propanol is as follows: TBAB:AP > TBAC:AP > TEAC:AP, which seems to suggest that the melting temperature of salt may influence the melting temperature of deep eutectic solvents. Besides, the highest values of T_m are observed for tetrabutylammonium bromide based DESs, which T_m is greater than that of TBAC. Moreover, the comparison of the melting temperatures for DES containing tetrabutylammonium and tetraethylammonium chlorides leads to the conclusion, that the melting temperature of deep eutectic solvents increases with increasing cation alkyl chain length in the salt and T_m of salt itself.

3.2. Density

3.2.1. Experimental values

The density, viscosity, refractive index and sound velocity of the deep eutectic solvents studied were measured as a function of temperature with the range of 293.15–333.15 K and at ambient pressure. The density data are presented in Table S1 and in Fig. 3 (a,b,c).

As it can been observed, density decreases linearly with the temperature increase for all molar compositions of all nine DESs. Obviously, this is due to of the formation of larger intermolecular voids at higher temperatures, which increase the volume and decrease the density. The fitting parameters of linear equations ($d = a \cdot T + b$) correlating the effect of temperature on the density, obtained by least square analysis are listed in Table 3.

The order of density for DES at the same temperature and molar ratio of the salt to 3-amine-1-propanol is as follows: TBAB:AP (DES

Table 2
The abbreviation, molar mass, molar ratio, mass fraction, water content and melting point for chemicals used in this work.

DES		Salt		HBD		Molar ratio	Mass fraction[a]		Water content[b]	
Symbol	$M_{DES}/(g \cdot mol^{-1})$		$M_{salt}/(g \cdot mol^{-1})$		$M_{HBD}/(g \cdot mol^{-1})$	Salt: HBD	Salt	HBD		T_m/K
DES1	124.229	TBAB	322.37	AP	75.11	1:4	0.5155	0.4845	0.00066	277.34
DES2	110.405	TBAB	322.37	AP	75.11	1:6	0.4168	0.5832	0.00053	274.41
DES3	102.580	TBAB	322.37	AP	75.11	1:8	0.3488	0.6512	0.00054	276.02; 278.6
DES4	93.265	TEAC	165.71	AP	75.11	1:4	0.3650	0.6440	0.00156	272.37
DES5	88.072	TEAC	165.71	AP	75.11	1:6	0.2692	0.7308	0.00127	272.19
DES6	85.189	TEAC	165.71	AP	75.11	1:8	0.2164	0.7836	0.00125	271.81
DES7	115.834	TBAC	277.92	AP	75.11	1:4	0.4818	0.5182	0.00178	276.29
DES8	103.851	TBAC	277.92	AP	75.11	1:6	0.3792	0.6208	0.00121	273.91
DES9	97.696	TBAC	277.92	AP	75.11	1:8	0.3168	0.6832	0.00202	277.33

[a] The standard uncertainty of DES mass fraction composition is 0.0001.
[b] Water content of DESs in mass fraction determined by Karl Fisher titration with the standard uncertainty ±0.0001.

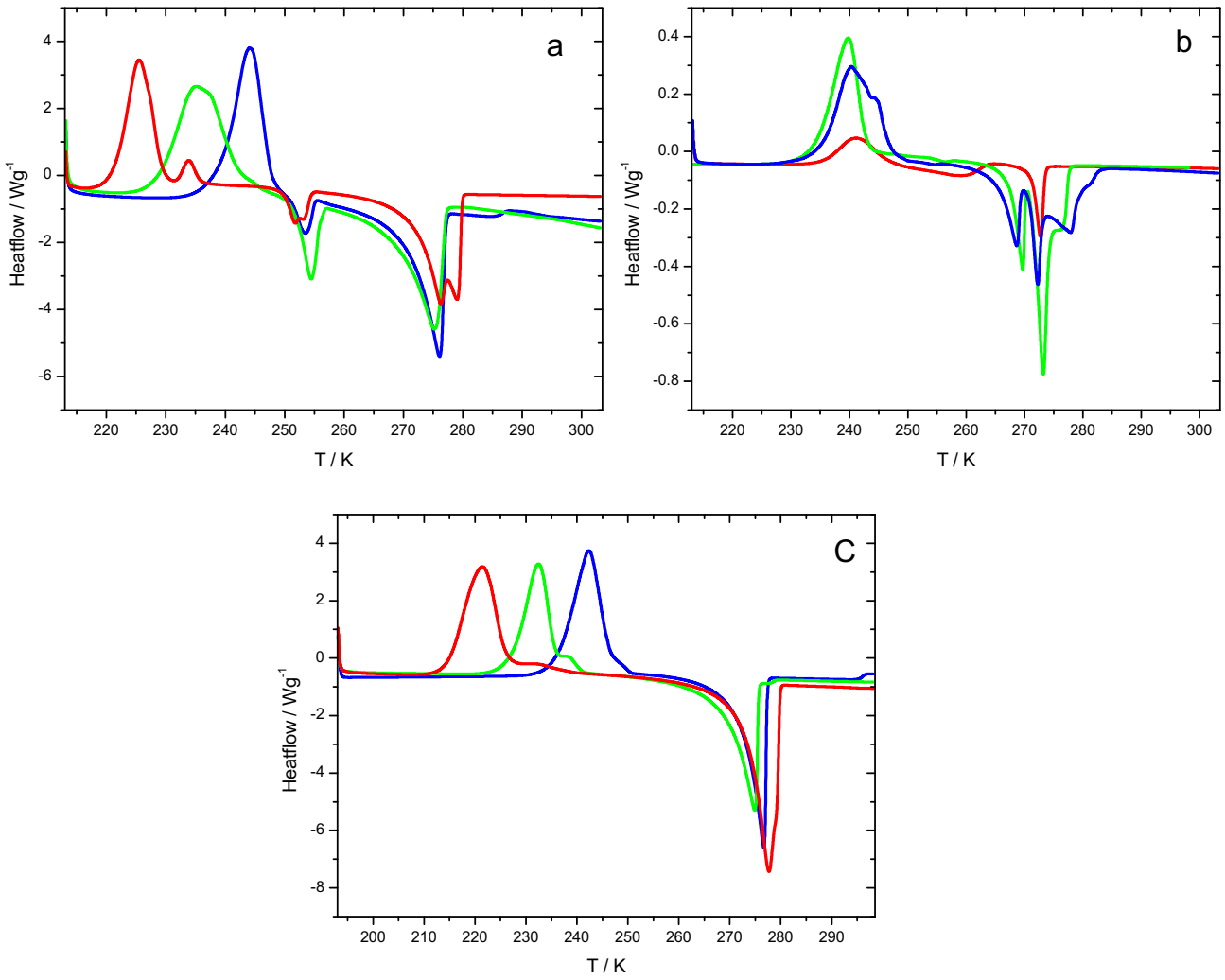

Fig. 2. DSC curves for deep eutectic solvents studied: a) TBAB:AP (DES 1–3), b) TEAC:AP (DES 4–6) and c) TBAC:AP (DES 7–9); (blue —1:4, red – 1:6, green 1:8). (For interpretation of the references to colour in this figure legend, the reader is referred to the web version of this article.)

1–3) > TEAC:AP (DES 4–6) > TBAC:AP (DES 7–9), which seems to suggest that structure of HBA as well as HBD may have a significant effect on the density values of deep eutectic solvents. The highest values of densities are observed for TBAB-based DESs, which is attributed to the mass of bromide being greater than chloride [16,17]. Moreover, comparing the density values for DES containing tetrabutylammonium and tetraethylammonium chlorides leads to conclusion, that the density of deep eutectic solvents decreases with the increasing cation alkyl chain length in the salt. That conclusion is consistent with the density results obtained for ILs [18,19]. Apparently, packing effects taking place in case of TBAB cause the increase of relative volume of salt and as a result the decrease of the density of DES. Moreover, the higher density values obtained for TBAB:AP (DES 1–3) than those for TEAC:AP (DES 4–6) suggest that the packaging effects have smaller influence on density than the effect connected with the mass of the anion.

As is seen from Table S1 and Fig. 3, the density of DESs also depends on the HBA:HBD molar ratio. For TBAB- and TEAC-based deep eutectic solvents, the density decreases with the increasing of molar ration of 3-amine-1-propanol, while for TBAC-based DESs the opposite trend is observed. Obviously, it is the result of different relation of density of deep eutectic solvents to the density of AP. The densities of TBAB:AP (DES 1–3) and TEAC:AP (DES 4–6) are higher than the density of pure 3-amine-1-propanol, while the density of TBAC:AP (DES 7–9) is lower. Thus, when the amount of 3-amine-1-propanol in TBAC:AP (DES 7–9) increases, the density tends to the smaller density of pure AP, i.e., it decreases.

3.2.2. Prediction of density values

Generally, three methods have been reported in the literature for estimating deep eutectic solvents densities so far. Shahbaz et al. used artificial intelligence and group contribution methods for density predictions in glycerol and ethylene glycol HBD components mixed with choline chloride, diethylethanolammonium chloride, and methyltriphenylphosphonium bromide as HBA components [20,21]. Mjalii introduced the mass connectivity index-based density prediction for a set of 20 deep eutectic solvents systems comprising different salts and hydrogen bond donors [22].

In the present study, the Rackett equation [23] modified by Spencer and Danner [24] and MCI-based (mass connectivity index-) density model [28] were used and their effectiveness for density prediction of DESs based on 3-amino-1-propanol were compared.

The first approach, i.e. the modified Racket equation, requires knowledge of critical temperature, critical volume and critical pressure of DESs. Because these parameters cannot be found experimentally, they are estimated using the Lee-Kesler mixing equations suggested by Knapp et al. [25]. Moreover, the Modified Lydersen-Joback-Reid method [26] is used to found the critical properties of components of deep eutectic solvents. The calculated critical properties of DESs obtained by using above methods are presented in Table 4.

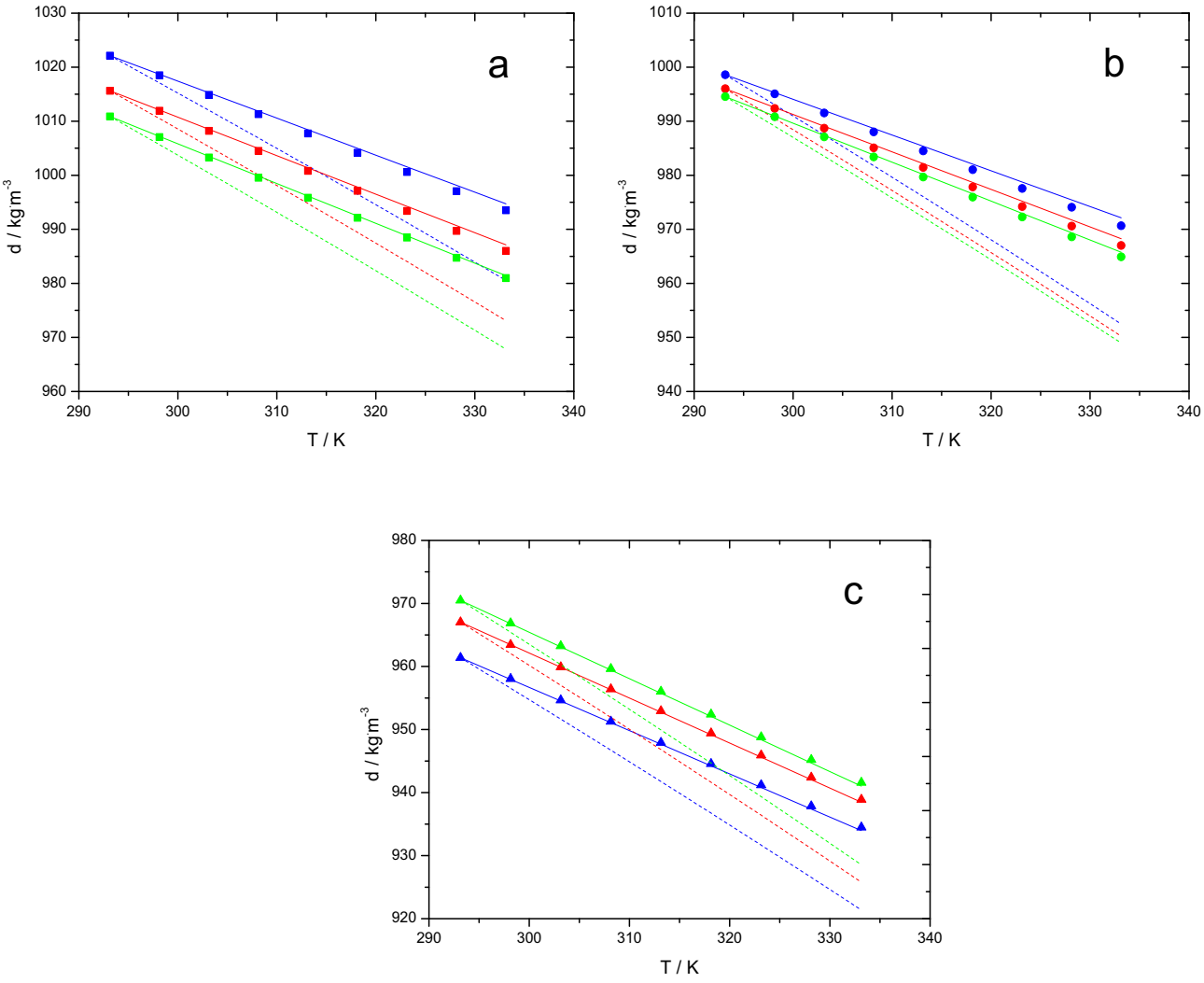

Fig. 3. Densities of deep eutectic solvents studied as a function of temperature in the range of 293.15–333.15 K and at atmospheric pressure a) TBAB:AP (DES 1–3), b) TEAC:AP (DES 4–6) and c) TBAC:AP (DES 7–9), (blue -1:4, red – 1:6, green 1:8); solid line – modified Racket equation, dashed line – mass connectivity index based method. (For interpretation of the references to colour in this figure legend, the reader is referred to the web version of this article.)

To predict the DES density the modified Rackett equation is employed as:

$$d = \frac{d_R}{Z_{RA}^{\varphi}} \tag{1}$$

where parameter φ is defined as

$$\varphi = \left(1-\frac{T}{T_{cm}}\right)^{2/7} - \left(1-\frac{T_R}{T_{cm}}\right)^{2/7} \tag{2}$$

and T_{cm}, d_R and T_R are critical temperature of DES, reference density and temperature, respectively. In the present study, the density at 293.15 K was chosen as the reference density. Z_{RA} is the specific compressibility factor introduced by Spencer and Danner to account for irregularities that cannot be handled by the original Racket model. It is defined as:

$$Z_{RA} = \left(\frac{V_{RS}\cdot P_{cm}}{R\cdot T_{cm}}\right)^{1/\left[1+\left(1-\frac{T}{T_{cm}}\right)^{2/7}\right]} \tag{3}$$

Table 3
Density model parameters along with root-mean-square deviations.

DES	a	b	RMSD	R^2
DES1	−0.715	1231.54	0.041	0.9999
DES2	−0.741	1232.71	0.050	0.9999
DES3	−0.745	1229.24	0.053	0.9999
DES4	−0.699	1203.31	0.051	0.9999
DES5	−0.725	1208.56	0.033	0.9999
DES6	−0.741	1211.72	0.028	0.9999
DES7	−0.673	1158.54	0.013	0.9999
DES8	−0.702	1172.88	0.030	0.9999
DES9	−0.722	1182.14	0.030	0.9999

Table 4
The calculated critical properties and mass connectivity indices of DESs used in this study and average relative deviation, where the superscript RA: Racket model, MCI: mass connectivity index- based model.

DES	T_{cm}/K	$10^3 V_{cm}/(m^3\cdot mol^{-1})$	P_{cm}/bar	MCI	ARD^{MCI} %	ARD^{RA} %
DES1	646.47	388.30	31.20	4.5320	0.07	0.62
DES2	636.61	350.02	34.18	5.6136	0.06	0.63
DES3	631.31	328.84	36.13	6.7102	0.03	0.64
DES4	607.30	317.12	36.81	3.7483	0.09	0.90
DES5	609.12	299.72	38.89	4.8440	0.07	0.83
DES6	620.25	290.19	40.14	5.9393	0.05	0.79
DES7	639.05	387.69	30.91	4.5323	0.03	0.68
DES8	630.91	347.90	34.10	5.6703	0.02	0.67
DES9	627.01	327.95	36.00	6.7241	0.03	0.66

where V_{SR} and P_{cm} are the saturated molar volume at the reference temperature and critical pressure of DES.

The second method applied in this study for the DESs density prediction, based on mass connectivity index, was introduced by Mjalli [22]. Using the training set of the experimental data consisting of 86 density values of DESs he found the semi-empirical equation for prediction of density as:

$$d(T) = d_R - 5.197 \cdot 10^{-4} \lambda_{DES}{}^{0.18293} (T - T_R) \quad (4)$$

in which λ_{DES} denotes to the mass connectivity index of DES, calculated on the basis of the pure components mass connectivity indices λ. Furthermore, the values of λ are estimated from equation [27]:

$$\lambda = \sum_{k=1}^{ij} \left(1/\sqrt{M_i M_j}\right) \quad (5)$$

where M_i and M_j are the masses of connected groups numbers (i) and (j) reported by Vaderrama et al. [28].

For 3-amine-1-propanol, tetrabutylammonium bromide, tetraethylammonium chloride and tetrabutylammonium chloride the mass connectivity indices were obtained as 0.5480, 2.3215, 1.5617 and 2.2515, respectively. Multiplying the salt and 3-amine-1-propanol mass connectivity indices by their molar quantities in the DES allowed us to calculate the mass connectivity indices of DESs, which are collected in Table 4.

Fig. 3 shows experimental and predicted densities of DESs based on 3-amino-1-propanol by the Rackett equation modified by Spencer and Danner and the model proposed by Mjalli. Moreover, the average relative deviations (ARD) between the experimental and models predicted densities are presented in Table 4. The negative variation of DES densities with temperature was captured by the Rackett equation, as well as by the MCI-based model. Moreover, the mass connectivity index model was successful in explaining this relationship with higher degree of credibility than the modified Rackett model. In all cases the Rackett predictions were underestimated with a much higher inclination with respect to temperature. The ARD values are the highest for deep eutectic solvents TEAC:AP (DES 4–6) and at the highest recorded temperature of 333.15 K are 1.87, 1.73, and 1.66% respectively. On the other hand, the MCI-based models gave ARD values of 0.15, 0.13 and 0.09% for the same systems. Thus, the obtained results indicate that the most proper method for density prediction for DESs is the method introduced by Mjalli [22].

3.2.3. Estimated thermodynamic properties of DESs

The isobaric thermal expansion coefficient α_p is defined as temperature dependence of ln(d) as expressed by the following equation:

$$\alpha_p = \frac{1}{V_m}\left(\frac{\partial V_m}{\partial T}\right)_p = -\left(\frac{\partial \ln(d)}{\partial T}\right)_p \quad (6)$$

where V_m and d are the molar volume and the density of DESs, respectively. It can be obtained by fitting the temperature dependence of ln (d) to the following straight line

$$\ln(d) = b - \alpha_p \cdot T \quad (7)$$

where b is an empirical constant. From Table 5 one can see, that α_p of DESs studied depend mainly on the molar ratio of the salt to 3-amine-1-propanol, while the dependence on the type of HBA is negligible. The smallest values of the thermal expansion coefficient were obtained for deep eutectic solvents containing the smallest amount of AP, suggesting the smallest free volumes or interstices in these solvents.

Table 5 presents also the molecular volume, standard molar entropy and lattice potential energy calculated from density at 298.15 K.

Table 5
Estimated physicochemical properties of DESs at 298.15 K at atmospheric pressure.

DES	$10^4\alpha/K^{-1}$	$V_{mol}/(nm^3)$	$S^o/(J{\cdot}K^{-1}{\cdot}mol^{-1})$	$U_{pot}/(kJ{\cdot}mol^{-1})$
DES1	7.09	0.203	281.8	503
DES2	7.40	0.181	255.1	518
DES3	7.48	0.169	240.1	528
DES4	7.10	0.156	223.3	540
DES5	7.39	0.147	213.0	548
DES6	7.56	0.143	207.3	553
DES7	7.10	0.201	279.6	504
DES8	7.37	0.179	252.4	520
DES9	7.42	0.168	238.6	529

Standard molar entropy and lattice potential energy of the studied DESs were estimated by using the empirical equations [29]:

$$S^o = 1246.5 \cdot V_{mol} + 29.5 \quad (8)$$

$$U_{pot} = 1981.2 \cdot (d/M)^{1/3} + 103.8 \quad (9)$$

As is seen from Table 5, the DESs exhibit low lattice energy which is an underlying reason for their liquid state at room temperature (U_{pot}, CsI = 613 kJ mol^{-1}) [30].

3.3. Viscosity

The experimental dynamic viscosity data of the binary mixtures corresponding to the applied temperature range of 293.15–333.15 K are listed in Table S2 and presented in Fig. 4 (a,b,c). As expected, temperature plays an important role in viscosity, namely decrease of this parameter was observed at higher temperatures. Higher temperatures increase kinetic energy of the ions and molecules, and weaken the attractive forces between them, promoting their movement and contributing to decreasing viscosity [31].

At lower temperatures the viscosity of DESs decreases rapidly and asymptotically approaches a lower value at higher temperatures [32]. The following tendency was nocited TBAB:AP (DES 1–3) > TBAC:AP (DES 7–9) > TEAC (DES 4–6) for a corresponding molar ratio of the compounds. In this regard, liquids composed of salts with smaller cation (shorter hydrocarbon substituent) and anion manifest lower viscosity (weaker interactions and flow resistance). All binary mixtures showed higher values of viscosity in comparison to 1-amino-1-propanol. Moreover, a decrease of the mole fraction of the salt in the system (increase of the molar ratio salt:AP) resulted in the lower values of the dynamic viscosity. For example, the viscosity of TBAB–AP at 298.15 K decreased from 84.7 to 50.2 mPa·s when the molar ratio raised from 1:4 to 1:8. Analogous relations were observed in the literature [31].

The dynamic viscosity results were further fitted with the Arrhenius and Vogel-Fulcher-Tamman (VFT) equations:

$$\eta = \eta_\infty \, exp^{\frac{E_a}{R \cdot T}} \quad (10)$$

$$\eta = \eta_o \, exp^{\frac{b}{T - T_o}} \quad (11)$$

where η_∞, E_a/R, η_0, b, and T_o are fitting parameters, η_∞ is the viscosity at infinite temperature, E_a is the activation energy, R is the gas constant, and T is the temperature in Kelvin. The fitting parameters determined from the experimental data along with root-mean-square deviations (RMSD) are presented in Tables 6 and 7. The E_a values calculated for the binary mixtures were found to vary from 33.4 kJ·mol^{-1} (DES 6) up to 38.5 kJ·mol^{-1} (DES 1), and reflect the abovementioned viscosity relations. The higher E_a value, the harder ions move past each other due to the interactions occurring in the fluid. DESs with the lowest salt: AP molar ratio (1:4) have higher activation energies. Based on the

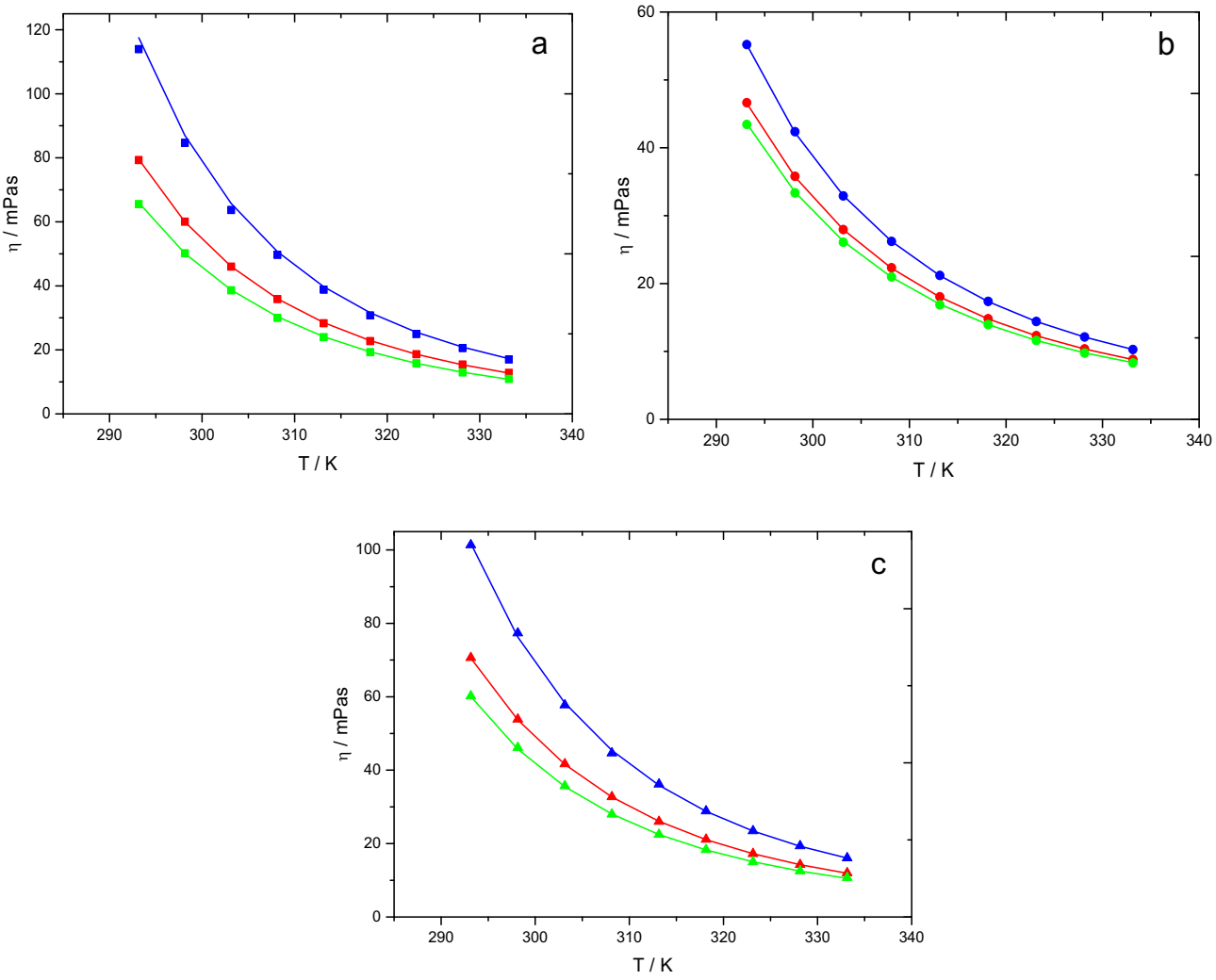

Fig. 4. Viscosities of deep eutectic solvents studied as a function of temperature in the range 293.15–333.15 K and at atmospheric pressure a) TBAB:AP (DES 1–3), b) TEAC:AP (DES 4–6) and c) TBAC:AP (DES 7–9), (blue -1:4, red – 1:6, green 1:8); solid line - Vogel-Fulcher-Tamman equation. (For interpretation of the references to colour in this figure legend, the reader is referred to the web version of this article.)

comparison of the correlation coefficients, R^2, and RMSD it was concluded that the VFT equation represents better fitting for the dynamic viscosity results.

3.4. Refractive index

3.4.1. Experimental values

The refractive index values of deep eutectic solvents studied at the temperature range from 293.13 to 333.15 K are presented in Table S3 and the trends are shown in Fig. 5 (a,b,c). There are several factors that have an effect on the refractive index of DESs such as type of salt, molar ratio of HBD to HBA, temperature and molecular weight of DES. The obtained results reveal that for all mixtures the values of refractive index decrease linearly with increasing the temperature. Adequate regression parameters ($n_D = a \cdot T + b$) are collected in Table 8.

Moreover, for a given temperature and molar ratio of salt to 3-amine-1-propanol, n_D value of the DESs is in the following order: TBAB:AP (DES 1–3) > TEAC:AP (DES 4–6) > TBAC:AP (DES 7–9), which is consistent with the order of density. Also, as the molecular weight of DESs decreases (see values of n_D for TBAB- and TBAC-based DESs),

Table 6
Fitting parameters for the Arrhenius equation for dynamic viscosity results determined within temperature range $T = (293.15$ to $333.15)$ K and $P = 0.1$ MPa.

DES	$10^5\eta_\infty$/mPa·s	10^{-4} E_a/J·mol^{-1}	RMSD	R^2
DES1	1.47	3.85	0.025	0.9984
DES2	1.98	3.70	0.023	0.9986
DES3	1.97	3.65	0.020	0.9988
DES4	4.62	3.40	0.024	0.9980
DES5	4.42	3.37	0.024	0.9981
DES6	4.58	3.34	0.024	0.9981
DES7	2.20	3.73	0.026	0.9982
DES8	2.60	3.60	0.020	0.9989
DES9	3.14	3.51	0.025	0.9980

Table 7
Fitting parameters for the Vogel-Fulcher-Tamman (VFT) equation, for dynamic viscosity results determined within temperature range $T = (293.15$ to $333.15)$ K and $P = 0.1$ MPa.

DES	η_0/mPa·s	b/K	T_0/K	RMSD	R^2
DES1	0.0316	1080.7	161.7	0.025	0.9999
DES2	0.0175	1214.0	149.0	0.011	0.9999
DES3	0.0086	1411.1	135.4	0.019	0.9999
DES4	0.0600	835.6	170.7	0.0025	0.9999
DES5	0.0539	827.9	170.7	0.0010	0.9999
DES6	0.0550	811.3	171.6	0.0023	0.9999
DES7	0.0311	1094.6	157.9	0.025	0.9997
DES8	0.0153	1261.6	143.6	0.0031	0.9999
DES9	0.0289	1034.7	157.7	0.013	0.9999

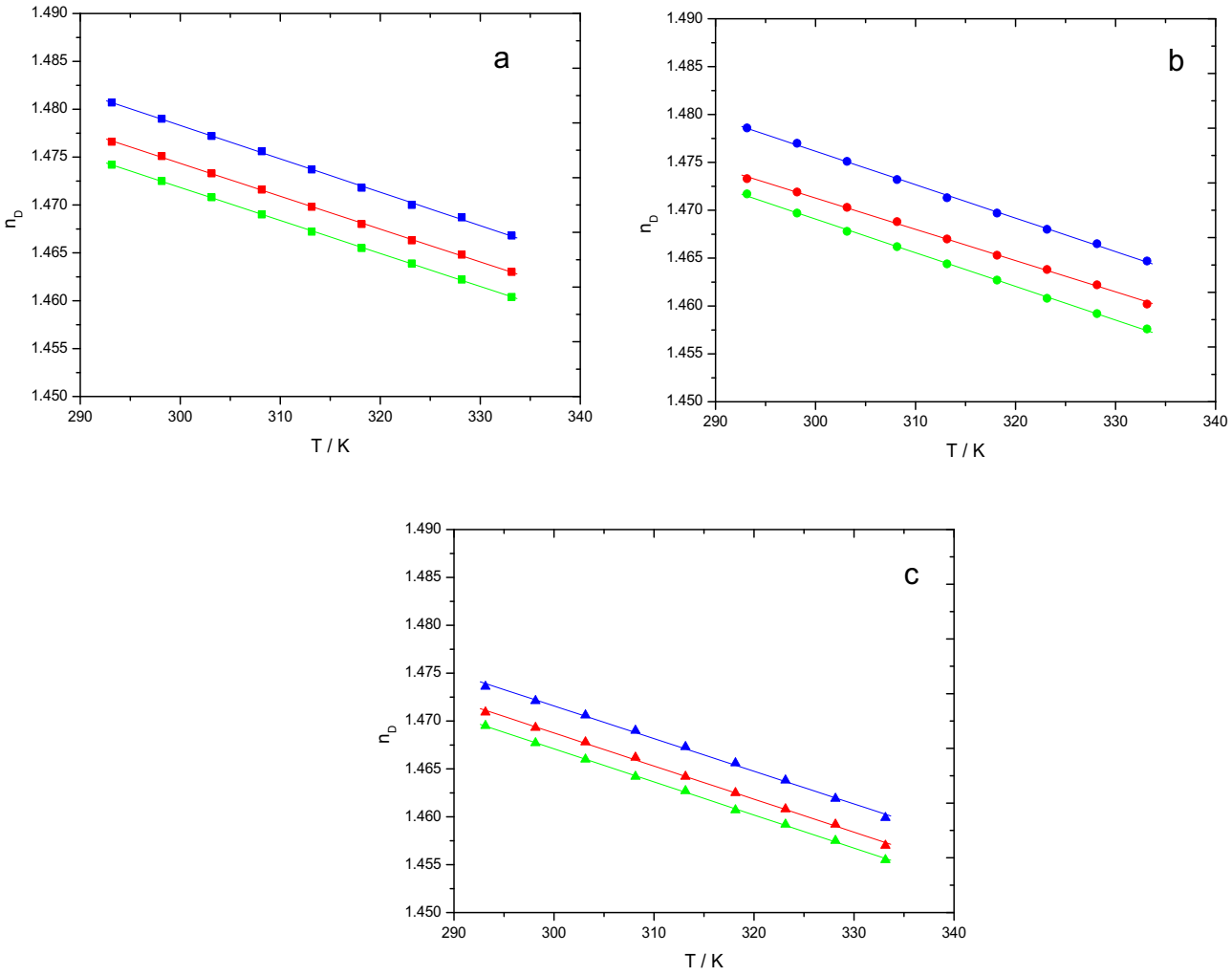

Fig. 5. Refractive indices of deep eutectic solvents studied as a function of temperature in the range 293.15–333.15 K a) TBAB:AP (DES 1–3), b) TEAC:AP (DES 4–6) and c) TBAC:AP (DES 7–9), (blue -1:4, red – 1:6, green 1:8), solid line –linear fit. (For interpretation of the references to colour in this figure legend, the reader is referred to the web version of this article.)

the value of refractive index of deep eutectic solvents decreases at all temperatures. As it was observed for viscosities, the refractive indices decrease with an increasing of mole fraction of AP in the mixture for all DESs investigated. Obviously, it is the result of the smaller value of the refractive index of 3-amine-1-propanol comparing to that of deep eutectic solvents. Thus, when the content of AP increases in DES, the refractive index decreases.

3.4.2. Prediction of refractive index values

It is generally accepted that the atomic contribution method is more accurate than others in predicting the refractive indices of organic liquids [33]. In this method molar refraction of compound is calculated by summing its atomic and structural contribution parameters, which were determined by Wildman and Crippen using 3412 molecules data set [34]. Then, Lorentz–Lorenz equation and experimental density value of compound is employed to calculate the refractive index:

$$R_M = \frac{M}{d}\left(\frac{n^2-1}{n^2+2}\right) \tag{12}$$

In this equation R_M, M ($g \cdot mol^{-1}$) and d ($g \cdot cm^{-3}$) are molar refraction, molar mass and density, respectively.

In the present study, the molar refractions of pure components of DESs, i.e., the salts and 3-amine-1-propanol were initially calculated and they were found to be equal to 0.757, 87.564, 47.557 and 84.493 for AP, TBAB, TEAC and TBAC, respectively. Then, molar refraction of DESs were obtained through equation:

$$R_M = \sum x_i R_{Mi} \tag{13}$$

where x_i and R_{Mi} are mole fraction and molar refraction of the individual constituting salt and AP. Finally, the refractive indices were calculated by Lorentz-Lorenz equation using the experimental values of density.

Table 9 presents the calculated molar refractions and the refractive indices for all DESs together with the experimental values and relative deviations at 293.15 K. As it can be seen, the predicted data of DESs molar refractions and refractive indices are in good agreement with the experimental data. Specially, the value of ARD% obtained for refractive indices equal to 0.41% confirms that the atomic contributions

Table 8
Refractive index model parameters and regression coefficients.

DES	a	b	RMSD	R^2
DES1	−0.00035	1.5830	0.00015	0.9992
DES2	−0.00034	1.5772	0.000098	0.9998
DES3	−0.00034	1.5752	0.000063	0.9990
DES4	−0.00035	1.5810	0.00017	0.9990
DES5	−0.00033	1.5693	0.00016	0.9989
DES6	−0.00035	1.5745	0.00014	0.9993
DES7	−0.00034	1.5740	0.00025	0.9977
DES8	−0.00035	1.5723	0.00020	0.9985
DES9	−0.00035	1.5708	0.00012	0.9995

Table 9
Calculated molar refractions and predicted refractive indices of DESs at 293.15 K.

DES	$R_{M\ exp}$	$R_{M\ cal}$	%RD	n_{exp}	n_{cal}	%RD
DES1	34.570	34.029	1.57	1.4807	1.4719	0.59
DES2	30.691	30.293	1.30	1.4766	1.4694	0.49
DES3	28.522	28.170	1.24	1.4742	1.4674	0.47
DES4	26.465	26.128	1.28	1.4786	1.4715	0.49
DES5	24.819	24.591	1.47	1.4733	1.4682	0.35
DES6	23.972	23.739	0.98	1.4717	1.4664	0.37
DES7	33.838	33.556	0.84	1.4736	1.4690	0.32
DES8	30.012	29.790	0.75	1.4709	1.4668	0.28
DES9	28.061	27.855	0.74	1.4695	1.4655	0.28
ARD%			1.13			0.41

method can be considered as the suitable method for the prediction of n_D values of DESs, though the atomic contributions proposed by Wildman and Crippen were considered for neutral compounds [34].

3.5. Sound velocity

The experimental sound velocity data for all DESs as a function of temperature are summarized in Table S4 and presented in Fig. 6 (a,b, c). As it can be seen, the sound velocity, similarly to other properties, decreases with increasing temperature. This behaviour was also reported in case of other DESs. At elevated temperature the molecules move further apart from each other, generating more free space and in the result density, viscosity, refractive index and sound velocity decrease [35–37]. Moreover, similar to most other DESs, the sound velocity of DESs investigated in the present study shows linear relationship with the temperature. Table 10 shows regression parameters ($u = a \cdot T + b$). Previously, the temperature dependence of the speed of sound was found to be nonlinear only for deep eutectic solvents based on benzyltrimethylammonium chloride and benzyltributylammonium chloride as HBAs and glycerol HBD, as well as deep eutectic solvents based on L-proline [38].

As is seen from Table 10, for a given temperature and molar ratio of salt to 3-amine-1-propanol, sound velocity of the DESs is in the following order: TEAC:AP ≫ TBAC:AP > TBAB:AP, which is opposite with the order of viscosity. Moreover, values of sound velocity obtained for TEAC-based DESs are significantly higher than those for TBAC- or TBAB-based DESs, which are similar in their magnitude. This result indicates that sound velocity is mainly determined by alkyl chain length of the HBD, while the type of anion has much smaller influence on it. Obviously, the less compact structure of TBAC:AP (DES 7–9) compared to that of TEAC:AP (DES 4–6) results in significantly smaller sound velocity value.

The sound velocity of the DESs similarly to other physical properties also depends on the molar ratio of HBA to HBD. For TBAB- and TBAC-based deep eutectic solvents sound velocity increases with increasing of molar ratio of 3-amine-1-propanol, while for TEAC-based DES the opposite trend is observed. Obviously, it is the result of different relation of the physical property of deep eutectic solvents to that of AP.

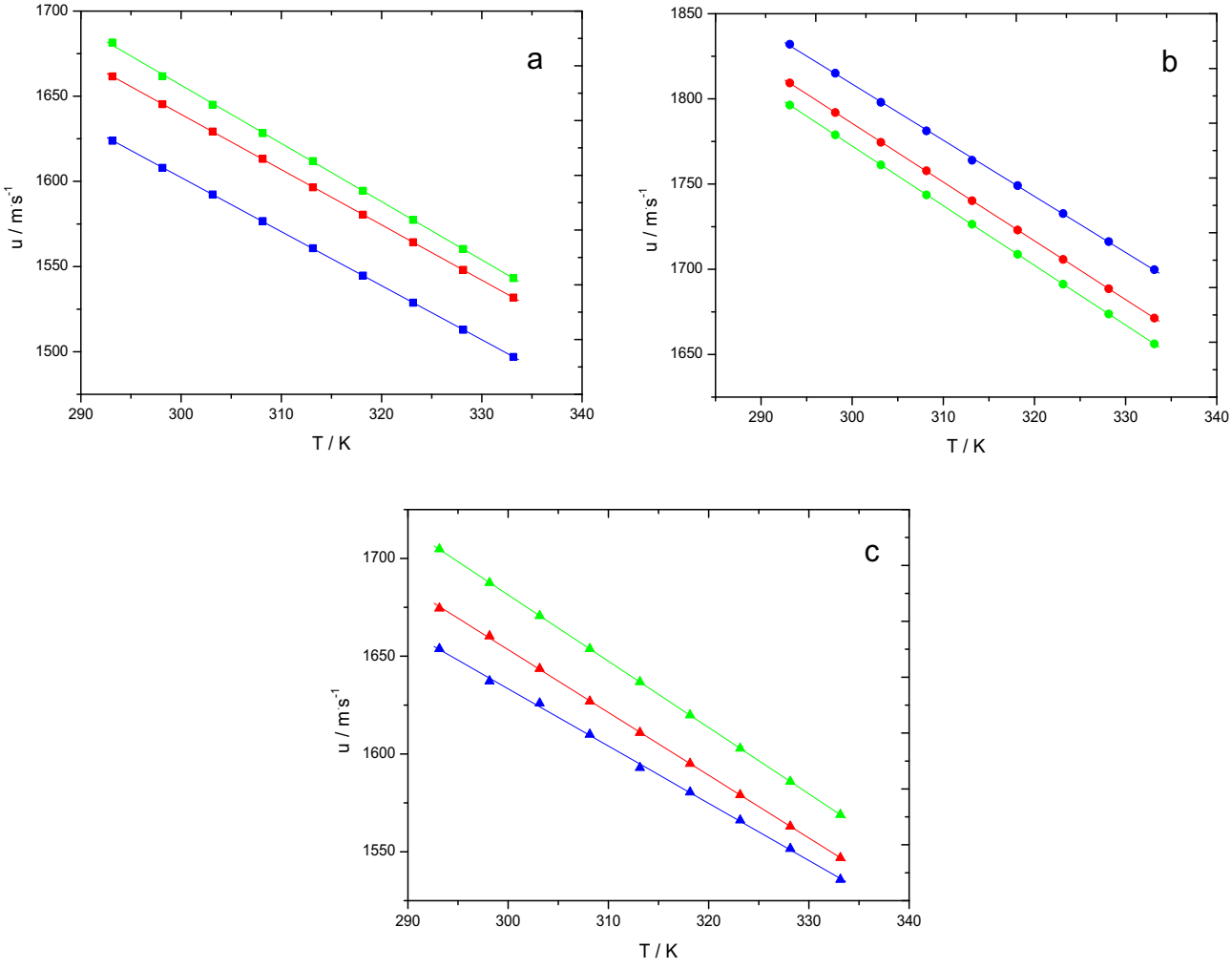

Fig. 6. Sound velocities of deep eutectic solvents studied as a function of temperature in the range 293.15–333.15 K a) TBAB:AP (DES 1–3), b) TEAC:AP (DES 4–6) and c) TBAC:AP (DES 7–9) (blue -1:4, red – 1:6, green 1:8), solid line –linear fit. (For interpretation of the references to colour in this figure legend, the reader is referred to the web version of this article.)

Table 10
Sound velocity model parameters and regression coefficients.

DES	a	b	RMSD	R^2
DES1	−3.17	2554.5	0.20	0.9999
DES2	−3.25	2613.5	0.20	0.9999
DES3	−3.42	2682.7	0.90	0.9997
DES4	−3.29	2796.9	0.80	0.9998
DES5	−3.45	2820.0	0.20	0.9999
DES6	−3.50	2823.3	0.10	0.9999
DES7	−2.93	2511.5	1.3	0.9992
DES8	−3.21	2616.3	0.60	0.9999
DES9	−3.39	2698.9	0.10	0.9999

3.5.1. Isentropic compressibility

Based on the experimental values of sound velocity and density, the technologically important parameter of isentropic compressibility was estimated. It was calculated by applying the Newton-Laplace equation:

$$\kappa_S = \frac{1}{\rho \cdot u^2} \tag{14}$$

The isentropic compressibility also gives a measure of the available free space in the liquid. From the calculated values reported in Table S5, it is observed that the κ_s changes with the increase of the temperature or increase of the amount of AP in DES in opposite trend than for that noticed for sound velocity. The smallest values of isentropic compressibility were observed for TEAC:AP (DES 4–6) for which the most compact structure is expected.

3.6. FTIR analysis of the DESs

Infrared spectroscopy is an invaluable tool for studying intermolecular interactions of aminoalcohol-based DESs [11]. The FTIR spectra of the studied DESs are shown in Fig. 7 together with the reference of pure AP spectrum.

The bands in the AP spectrum were previously ascribed in great detail [39]. The region of particular interest here is the ν(OH)/ν(NH_2) stretching vibrations range (3000–3600 cm^{-1}), distinctly sensitive to the hydrogen bonding. Pure AP is an associated liquid with as many as four hydrogen bonds formed per molecule [40] as found in molecular dynamics simulations. In DES, some of the internal hydrogen bonds are replaced by aminoalcohol to halide bonding. In water, such bonds are slightly weaker than water–water hydrogen bonds [41]. In the studied DESs, the dominant effect in the IR spectrum is the lowering of the intensity of all the AP bands due to the lower concentration of aminoalcohol. At the same time, positions of the ν(OH)/ν(NH_2) bands become slightly blue-shifted due to the emergence of OH–halide and NH–halide hydrogen bonds. Interestingly, the ν(OH) band at 3171 cm^{-1} is apparently much more perturbed by the formation of DES than the doublet of symmetric/asymmetric ν(NH_2) bands at 3288/3347 cm^{-1}, indicating it is a much more sensitive probe of the intermolecular interactions in the synthesized DESs.

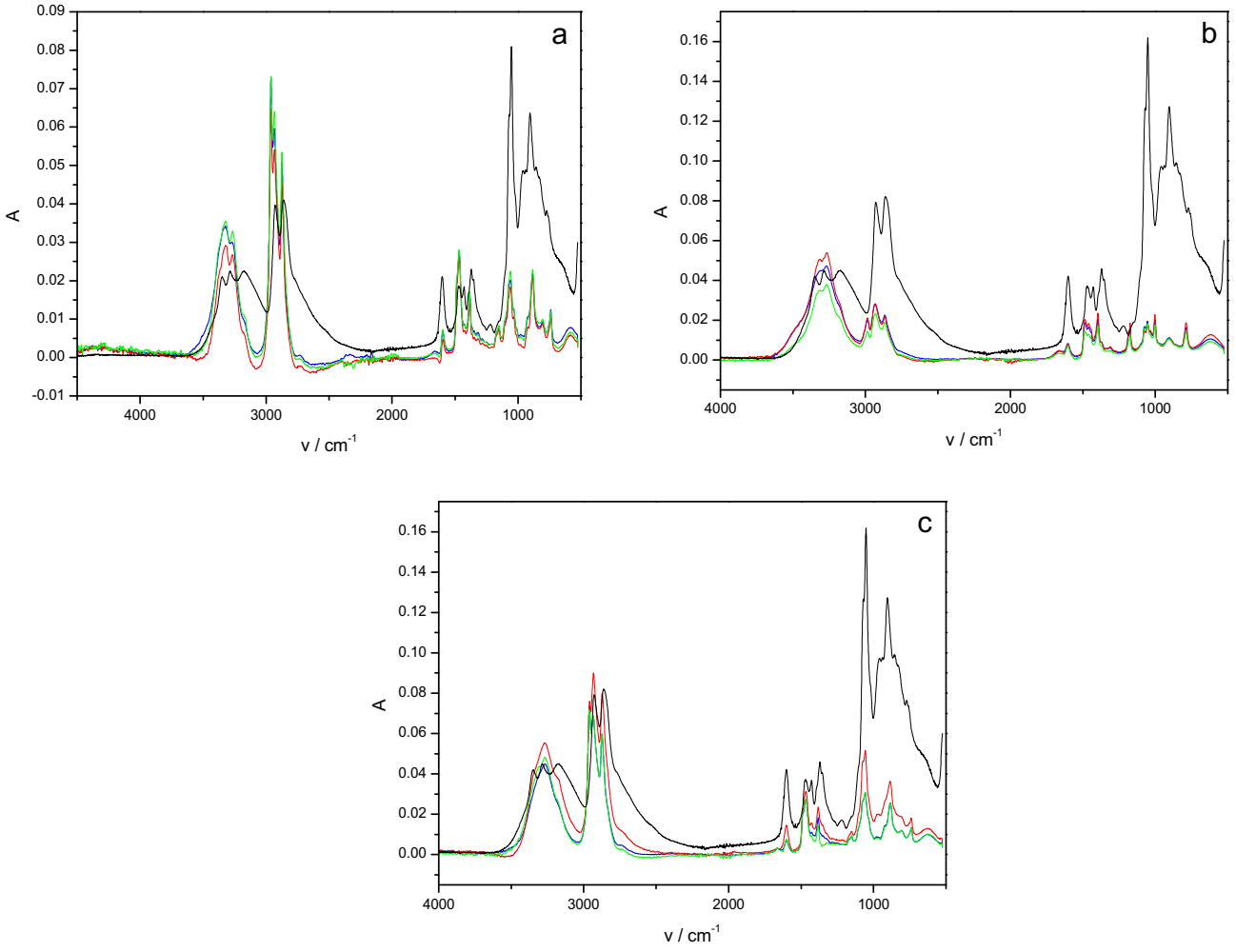

Fig. 7. The FTIR spectra of the studied DESs together with the pure AP spectrum; a) TBAB:AP (DES 1–3), b) TEAC:AP (DES 4–6) and c) TBAC:AP (DES 7–9) (blue -1:4, red – 1:6, green 1:8). (For interpretation of the references to colour in this figure legend, the reader is referred to the web version of this article.)

Below 1500 cm^{-1}, the intramolecular bands of the tetraalkylammonium cations are superimposed on the solvent background. Comparison with the pure salts (see Fig. S1), but note that spectra of some of the salts were difficult to record in an anhydrous state, reveals neither changes in band positions, nor formation of any new bands, thus confirming the lack of specific chemical interactions between the DESs components.

4. Conclusions

Experimental density, viscosity, refractive index and sound velocity for 3-amino-1-propanol plus tetrabutylammonium bromide, 3-amino-1-propanol plus tetraethylammonium chloride and 3-amino-1-propanol plus tetrabutylammonium chloride deep eutectic solvents with different molar ratios of 1:4, 1:6 and 1:8 salt to AP have been reported as a function of temperature at atmospheric pressure. From the experimental data, the thermal expansion coefficients, the activation energies for viscous flow and the isentropic compressibility of DESs were calculated.

It was found that density, refractive index and sound velocity of the studied deep eutectic solvents decrease linearly with temperature, while viscosity changes exponentially with temperature. The Vogel-Tamman-Fulcher equation better describes the dependence of viscosity on temperature than the Arrhenius equation.

Furthermore, the results revealed that the order of density and refractive index for DESs at the same temperature and molar ratio of the salt to 3-amine-1-propanol is as follows: TBAB:AP (DES 1–3) > TEAC:AP (DES 4–6) > TBAC:AP (DES 7–9), while the smallest values of viscosity and isentropic compressibility for TEAC:AP (DES 4–6) are observed.

Rackett equation modified by Spencer and Danner and the mass connectivity index-based method used for density prediction indicate that the most proper method for density prediction for the selected deep eutectic solvents is the method introduced by Mjalli. Moreover, the value of ARD% obtained for refractive indices equal to 0.41% confirms that the atomic contributions method can be considered as the suitable method to prediction of n_D of DESs.

To sum up the study, taking into account physical properties, especially viscosity, deep eutectic solvent composed of tetraethylammonium chloride and 3-amino-1-propanol appears to be the best solvent among those considered for use as an absorbent of carbon dioxide.

CRediT authorship contribution statement

Bartosz Nowosielski: Investigation, Formal analysis, Data curation, Writing - review & editing.**Marzena Jamrógiewicz:**Investigation, Formal analysis, Data curation, Writing - original draft, Writing - review & editing.**Justyna Łuczak:**Investigation, Formal analysis, Data curation, Writing - original draft, Writing - review & editing.**Maciej Śmiechowski:**Investigation, Formal analysis, Data curation, Writing - original draft, Writing - review & editing.**Dorota Warmińska:**Conceptualization, Investigation, Formal analysis, Data curation, Writing - original draft, Writing - review & editing.

Declaration of competing interest

The authors declare that they have no known competing financial interests or peisonal relationships that could have appeared to influence the work reported in this paper.

Appendix A. Supplementary data

Supplementary data to this article can be found online at https://doi.org/10.1016/j.molliq.2020.113110.

References

[1] N. Du, et al., Polymer nanosieve membranes for CO2-capture applications, Nat. Mater. 10 (5) (2011) 372–375.
[2] G.T. Rochelle, Amine scrubbing for CO2 capture, Science (80-.) 325 (5948) (2009) 1652–1654.
[3] X. Li, M. Hou, B. Han, X. Wang, L. Zou, Solubility of CO2 in a choline chloride + urea eutectic mixture, J. Chem. Eng. Data 53 (2) (2008) 548–550.
[4] Y. Marcus, Deep Eutectic Solvents, Springer International Publishing, 2019.
[5] S. Sarmad, J.P. Mikkola, X. Ji, Carbon dioxide capture with ionic liquids and deep eutectic solvents: a new generation of sorbents, ChemSusChem 10 (2) (2017) 324–352.
[6] I. Adeyemi, M.R.M. Abu-Zahra, I. Alnashef, Experimental study of the solubility of CO2in novel amine based deep eutectic solvents, Energy Procedia 105 (2017) 1394–1400.
[7] T.J. Trivedi, J.H. Lee, H.J. Lee, Y.K. Jeong, J.W. Choi, Deep eutectic solvents as attractive media for CO2 capture, Green Chem. 18 (9) (2016) 2834–2842.
[8] S.K. Shukla, J.P. Mikkola, Intermolecular interactions upon carbon dioxide capture in deep-eutectic solvents, Phys. Chem. Chem. Phys. 20 (38) (2018) 24591–24601.
[9] H. Ghaedi, et al., Density, excess and limiting properties of (water and deep eutectic solvent) systems at temperatures from 293.15 K to 343.15 K, J. Mol. Liq. 248 (2017) 378–390.
[10] I. Adeyemi, M.R.M. Abu-Zahra, I. Alnashef, Novel green solvents for CO2 capture, Energy Procedia 114 (2017) 2552–2560.
[11] F.S. Mjalli, G. Murshid, S. Al-Zakwani, A. Hayyan, Monoethanolamine-based deep eutectic solvents, their synthesis and characterization, Fluid Phase Equilib. 448 (2017) 30–40.
[12] I. Adeyemi, M.R.M. Abu-Zahra, I.M. AlNashef, Physicochemical properties of alkanolamine-choline chloride deep eutectic solvents: measurements, group contribution and artificial intelligence prediction techniques, J. Mol. Liq. 256 (2018) 581–590.
[13] M.B. Haider, D. Jha, B. Marriyappan Sivagnanam, R. Kumar, Thermodynamic and kinetic studies of CO2 capture by glycol and amine-based deep eutectic solvents, J. Chem. Eng. Data 63 (8) (2018) 2671–2680.
[14] E. Ali, et al., Solubility of CO2 in deep eutectic solvents: experiments and modelling using the Peng-Robinson equation of state, Chem. Eng. Res. Des. 92 (10) (2014) 1898–1906.
[15] A.P. Abbott, G. Capper, D.L. Davies, R.K. Rasheed, V. Tambyrajah, Novel solvent properties of choline chloride/urea mixtures, Chem. Commun. 9 (1) (2003) 70–71.
[16] E.L. Smith, A.P. Abbott, K.S. Ryder, Deep eutectic solvents (DESs) and their applications, Chem. Rev. 114 (21) (2014) 11060–11082.
[17] Q. Zhang, K. De Oliveira Vigier, S. Royer, F. Jérôme, Deep eutectic solvents: syntheses, properties and applications, Chem. Soc. Rev. 41 (21) (2012) 7108–7146.
[18] T.L. Greaves, A. Weerawardena, C. Fong, I. Krodkiewska, C.J. Drummond, Protic ionic liquids: solvents with tunable phase behavior and physicochemical properties, J. Phys. Chem. B 110 (45) (2006) 22479–22487.
[19] S.B. Capelo, et al., Effect of temperature and cationic chain length on the physical properties of ammonium nitrate-based protic ionic liquids, J. Phys. Chem. B 116 (36) (2012) 11302–11312.
[20] K. Shahbaz, S. Baroutian, F.S. Mjalli, M.A. Hashim, I.M. Alnashef, Densities of ammonium and phosphonium based deep eutectic solvents: prediction using artificial intelligence and group contribution techniques, Thermochim. Acta 527 (2012) 59–66.
[21] K. Shahbaz, F.S. Mjalli, M.A. Hashim, I.M. Alnashef, Prediction of deep eutectic solvents densities at different temperatures, Thermochim. Acta 515 (1–2) (2011) 67–72.
[22] F.S. Mjalli, Mass connectivity index-based density prediction of deep eutectic solvents, Fluid Phase Equilib. 409 (2016) 312–317.
[23] H.G. Rackett, Equation of state for saturated liquids, J. Chem. Eng. Data 15 (4) (1970) 514–517.
[24] C.F. Spencer, R.P. Danner, Improved equation for prediction of saturated liquid density, J. Chem. Eng. Data 17 (2) (1972) 236–241.
[25] H. Knapp, R. Doring, L. Oellrich, U. Plocker, J.M. Prausnitz, Vapor-liquid Equilibria for Mixtures of Low Boiling Substances, Chemistry Data Series, VI, , DECHEMA, Frankfurt, Ger. 1982, 1982.
[26] V.H. Alvarez, J.O. Valderrama, A modified Lydersen-Joback-Reid method to estimate the critical properties of biomolecules, Alimentaria 254 (2004) 55–66.
[27] M. Randić, On characterization of molecular branching, J. Am. Chem. Soc. 97 (23) (1975) 6609–6615.
[28] J.O. Valderrama, R.E. Rojas, Mass connectivity index, a new molecular parameter for the estimation of ionic liquid properties, Fluid Phase Equilib. 297 (1) (2010) 107–112.
[29] L. Glasser, Lattice and phase transition thermodynamics of ionic liquids, Thermochim. Acta 421 (1–2) (2004) 87–93.
[30] D.R. Lide, CRC Handbook of Chemistry and Physics, 85, CRC press, 2004.
[31] S. Sarmad, Y. Xie, J.P. Mikkola, X. Ji, Screening of deep eutectic solvents (DESs) as green CO2 sorbents: from solubility to viscosity, New J. Chem. 41 (1) (2017) 290–301.
[32] M.H. Ghatee, M. Zare, F. Moosavi, A.R. Zolghadr, Temperature-dependent density and viscosity of the ionic liquids 1-alkyl-3-methylimidazolium iodides: experiment and molecular dynamics simulation, J. Chem. Eng. Data 55 (9) (2010) 3084–3088.
[33] X. Cao, B.C. Hancock, N. Leyva, J. Becker, W. Yu, V.M. Masterson, Estimating the refractive index of pharmaceutical solids using predictive methods, Int. J. Pharm. 368 (1–2) (2009) 16–23.
[34] S.A. Wildman, G.M. Crippen, Prediction of physicochemical parameters by atomic contributions, J. Chem. Inf. Comput. Sci. 39 (5) (1999) 868–873.

[35] D. Lapeña, L. Lomba, M. Artal, C. Lafuente, B. Giner, Thermophysical characterization of the deep eutectic solvent choline chloride:ethylene glycol and one of its mixtures with water, Fluid Phase Equilib. 492 (2019) 1–9.
[36] P.B. Sánchez, B. González, J. Salgado, J. José Parajó, Á. Domínguez, Physical properties of seven deep eutectic solvents based on L-proline or betaine, J. Chem. Thermodyn. 131 (2019) 517–523.
[37] A. Basaiahgari, S. Panda, R.L. Gardas, Acoustic, volumetric, transport, optical and rheological properties of Benzyltripropylammonium based deep eutectic solvents, Fluid Phase Equilib. 448 (2017) 41–49.
[38] A. Basaiahgari, S. Panda, R.L. Gardas, Effect of ethylene, diethylene, and triethylene glycols and glycerol on the physicochemical properties and phase behavior of benzyltrimethyl and benzyltributylammonium chloride based deep eutectic solvents at 283.15-343.15 K, J. Chem. Eng. Data 63 (7) (2018) 2613–2627.
[39] C. Cacela, M.L. Duarte, R. Fausto, Structural and vibrational characterization of 3-amino-1-propanol a concerted SCF-MO ab initio, Raman and infrared (matrix isolation and liquid phase) spectroscopy study, Spectrochim. Acta - Part A Mol. Biomol. Spectrosc 56 (6) (2000) 1051–1064.
[40] S.M. Melnikov, M. Stein, Molecular dynamics study of the solution structure, clustering, and diffusion of four aqueous alkanolamines, J. Phys. Chem. B 122 (10) (2018) 2769–2778.
[41] J. Stangret, T. Gampe, Ionic hydration behavior derived from infrared spectra in HDO, J. Phys. Chem. A 106 (21) (2002) 5393–5402.